Bistability in silicon microring resonator based on strain induced by a piezoelectric lead zirconate titanate thin film

Cite as: Appl. Phys. Lett. **100**, 141107 (2012); https://doi.org/10.1063/1.3701587
Submitted: 20 February 2012 . Accepted: 19 March 2012 . Published Online: 03 April 2012

Y. Sebbag, I. Goykhman, B. Desiatov, T. Nachmias, O. Yoshaei, M. Kabla, S. E. Meltzer, and U. Levy

Bistability in silicon microring resonator based on strain induced by a piezoelectric lead zirconate titanate thin film

Y. Sebbag,[1] I. Goykhman,[1] B. Desiatov,[1] T. Nachmias,[2] O. Yoshaei,[2] M. Kabla,[2] S. E. Meltzer,[2] and U. Levy[1,a)]
[1]*Department of Applied Physics, The Benin School of Engineering and Computer Science, The Center for Nanoscience and Nanotechnology, The Hebrew University of Jerusalem, Jerusalem 91904, Israel*
[2]*Micro System and Smart Technologies, RAFAEL Ltd., P.O.B. 2250, Haifa 31021, Israel*

(Received 20 February 2012; accepted 19 March 2012; published online 3 April 2012)

We demonstrate bistability in a submicron silicon optical phase shifter based on the photoelastic effect. The strain magnitude is electrically controlled by a piezoelectric thin film placed on top of the device. The hysteresis behavior of the piezoelectric response shows potential application as bistable device independent of the optical intensity. © *2012 American Institute of Physics*. [http://dx.doi.org/10.1063/1.3701587]

In recent years, cladding stress engineering in silicon-on-insulator (SOI) waveguides was investigated intensively, particularly focusing on the configuration of a rib waveguide with a cross-section of a few micrometers.[1] The stress applied to the waveguide changes the refractive index of the material via the photoelastic effect. In contrast to other effects generally used to change the refractive index in silicon, such as thermo-optic effect or free carrier dispersion effect, the photoelastic effect can be used to induce a relatively strong birefringence,[2] provided that the stress distribution is anisotropic. Indeed, engineering the stress distribution and its magnitude was used to control the total birefringence in micrometer sized cross-section waveguides. During recent years, stress engineering was utilized for the demonstration of various polarization independent devices,[3–5] and to induce a second-order susceptibility $\chi^{(2)}$ in silicon by breaking its crystal symmetry.[6,7] These approaches were based on passive stress engineering, using a passive stressing layer (typically oxide or nitride) on top of the waveguide. Dynamic control of the birefringence was also demonstrated using an integrated piezoelectric thin film layer as an electrically tunable stress transducer.[8] This active piezoelectric layer was used to achieve phase matching of nonlinear processes such as coherent anti-Stokes Raman scattering in silicon rib waveguide with cross section in the few micron regime.

Another important feature of nonlinear material response is the property of bistability. The property of bistability in optical devices can be used to realize optical logic gates or optical memories.[9] Generally, optical bistability is achieved by exploiting the nonlinear response of the material to the optical input power. Several techniques can be used to obtain bistable operation, including carrier-plasma dispersion, the optical Kerr effect, saturable absorption, and the thermo-optic effect. Relatively low optical power bistability in silicon chips was previously demonstrated using the strong field enhancement in optical micro-cavities.[10,11]

In this paper, we demonstrate bistability in a silicon optical phase-shifter by exploiting the nonlinear strain response of an electrically controlled piezoelectric stressing layer on top of the device. The nonlinear response of the piezoelectric material is transferred to the effective refractive index of the optical mode via the photoelastic effect. The efficiency of the photoelastic based phase-shifter depends on the design of the cladding layer's geometry while the bistability depends mostly on the intrinsic properties of the piezoelectric material.

The main advantage of this technique is that the bistability can be achieved regardless of the optical power. Moreover, since the nonlinear behavior has its origin in the piezoelectric top layer response, switching between different states does not involve changing the optical power.

The presented structure consists of a submicron ridge silicon waveguide with a silicon oxide clad, covered by a thin layer of lead zirconate titanate (PZT). PZT was chosen as the piezoelectric material because of its relatively large piezoelectric coefficient and its previous use in integrated micro-electro-mechanical systems (MEMS) and ferroelectric random-access memories (Fe-RAM) on silicon substrate.[12,13] The PZT layer is sandwiched between a top and a bottom electrode which are used to apply an electric field on the PZT. The thickness of the top oxide cladding layer is chosen to minimize the optical absorption losses resulted from the interaction of the bottom electrode of the PZT layer. We found that if the PZT layer is deposited on a flat surface, no stress would be transferred to the silicon waveguide, because the upper boundary of the PZT layer is free to move. In contrast, the presence of corners in the oxide cladding enables the transfer of the electrically tunable strain generated in the PZT layer into the silicon waveguide. As a result, the oxide layer is designed to have a cap above the core of the waveguide. The structure is shown schematically in Figure 1.

To optimize the structural parameters and evaluate the change in effective refractive index as a function of the applied voltage, we first performed computer simulations using a commercially available finite element analysis package (COMSOL Multiphysics) which includes piezoelectric, structural mechanics, and electromagnetic modules. The stress distribution resulting from the piezoelectric material was computed in the vicinity of the waveguide's core. Then, the change in the effective refractive index of the fundamental transverse electric (TE) waveguide mode was calculated.

a)Author to whom correspondence should be addressed. Electronic mail: ulevy@cc.huji.ac.il.

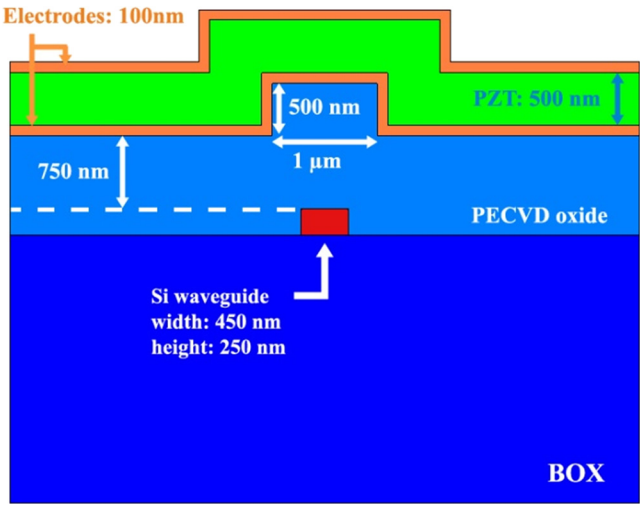

FIG. 1. Geometrical structure of the presented device.

The electromagnetic analysis showed that for a 450 nm wide and 250 nm high silicon waveguide, at a wavelength of 1.55 μm, the absorption losses due to the bottom electrode of the PZT layer are negligible if the thickness of the upper oxide cladding is about 1.25 μm on top of the silicon waveguide. Thus, we fixed the thickness of the oxide layer, above the waveguide to be 1.25 μm. Additionally, the thickness of the PZT layer was set to be 500 nm. The oxide cap was assumed to be 1 μm wide and 500 nm thick, centered around the middle of the silicon waveguide. The platinum (Pt) electrodes are 100 nm thick. The complex refractive index of Pt used in the simulation was[14]: $n = 5.31 + j7.04$. Thus, for the presented structure, the effective index of the fundamental TE mode, without stress, was found to be $n_{eff}^{TE} = 2.44 + j2.84 \times 10^{-8}$, corresponding to propagation loss of about 0.01 dB/cm, which is negligible compared to the propagation losses of the bare silicon waveguide, which are about 2 dB/cm.

Computer simulation results showing the stress distribution resulting from the piezoelectric material in the horizontal, σ_x, and vertical, σ_y, directions under an applied voltage of 5 V are shown in Figures 2(a) and 2(b), respectively.

The change in material's refractive index induced by the photoelastic effect can be expressed as[1]

$$\begin{aligned} \Delta n_x &= n_x - n_0 = -C_1 \times \sigma_x - C_2 \times (\sigma_y + \sigma_z), \\ \Delta n_y &= n_y - n_0 = -C_1 \times \sigma_y - C_2 \times (\sigma_x + \sigma_z), \end{aligned} \quad (1)$$

where n_x and n_y are the material's refractive index components obtained under the application of external electric field, n_0 is the bulk refractive index in the absence of stress, σ_x, σ_y, and σ_z are the relative stress tensor components, and C_1 and C_2 are the stress-optic (photoelastic) coefficients related to the Young's modulus, Poisson's ratio, and the photo-elastic tensor elements of the material. The new refractive index distribution was then used to simulate the change in the effective refractive index of the TE waveguide mode, Δn_{eff}^{TE}. Under an applied voltage of about 5 V on the PZT layer, a Δn_{eff}^{TE} of about 1×10^{-4} was obtained. For a slightly lower voltage level (4 V), Δn_{eff}^{TE} of about 9.1×10^{-5} was obtained.

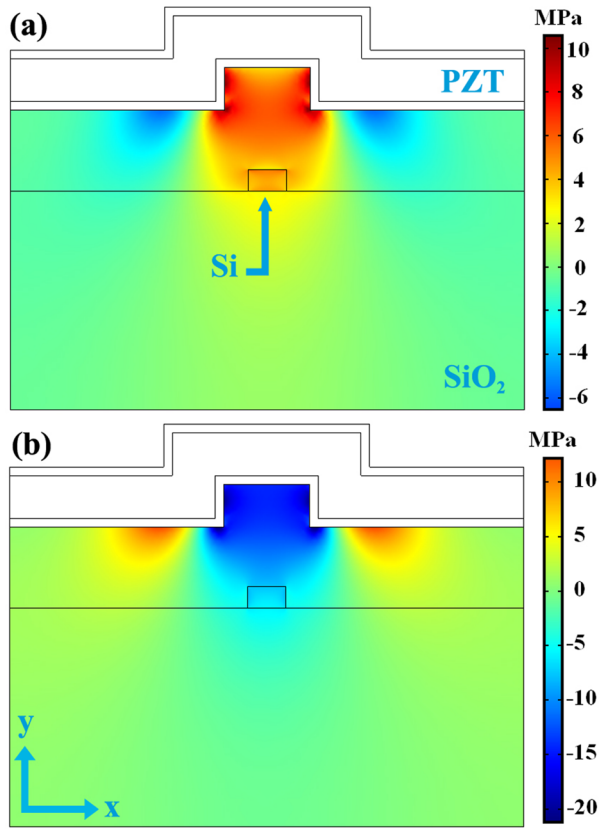

FIG. 2. Stress distribution in (a) the horizontal direction, σ_x, and (b) the vertical direction, σ_y, under an applied voltage of 5 V.

In order to experimentally demonstrate the proposed phase-shifter and its bistable property, a microring resonator consisting of the above discussed structure was fabricated. A SOI wafer with 250 nm thick upper silicon layer on top of 2 μm thick buried oxide layer was used to fabricate the optical device. The microring mask was patterned by electron-beam lithography (Raith e-line 150), and the pattern was transferred into the silicon device layer by the use of inductively coupled plasma (ICP) reactive ion etching (RIE) (Oxford Plasmalab 100). The device was then covered by 1.5 μm thick plasma enhanced chemical vapor deposition (PECVD) oxide layer. Next, a 1 μm wide cap pattern was defined by electron-beam lithography with precise alignment to the silicon waveguide. The pattern was transferred into the oxide layer by ICP RIE etching process (500 nm deep).

Following, the bottom electrode consisting of a Ti/Pt bilayer of 10 nm/100 nm thickness was deposited on the top oxide layer by evaporation. Next, a commercially available sol-gel morphotropic phase boundary $PZT - Zr/Ti = 52/48$ – (Inostek Inc.) thin film was successively spin-coated and dried until a 500 nm thick layer was obtained. The final annealing was done at 650 °C for 30 min to obtain crystallization. Then, the top electrode consisting of Cr/Au bilayer of 10 nm/100 nm was patterned by electron beam lithography and lift-off. Finally, the sol-gel PZT was poled at 50 °C for 10 min in order to enhance the piezoelectric response. Figure 3 presents an optical microscope top view micrograph of the fabricated structure with 20 μm ring radius and 200 nm coupling gap between the bus waveguide and the resonator.

The shift in the mode's effective refractive index results in a shift in the resonance wavelength of the microring. By

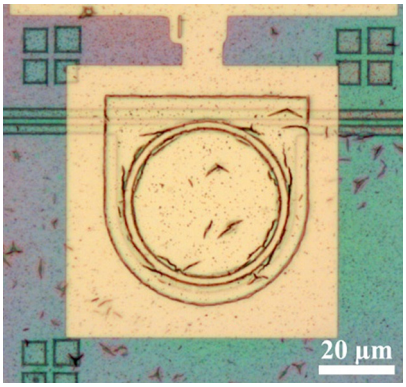

FIG. 3. Optical microscope photography top view of the fabricated microring resonator covered by the sol-gel PZT thin film sandwiched by the two electrodes.

tracking the resonance wavelength peak, one can evaluate the refractive index change. It can be approximated by the equation: $\Delta\lambda/\lambda_0 = \Delta n_{eff}/n_{eff}$, where λ_0 is the resonance wavelength without stress, and n_{eff} is the effective refractive index at this wavelength. Figure 4 shows the transmission spectrum of the microring under different applied voltages. The change in the effective refractive index was measured to be about $5.3 \times 10^{-5} \pm 5 \times 10^{-6}$ and about 1.8×10^{-4} under an applied voltage of 4 V and 6 V, respectively. These measurements seem to be in agreement with the simulations, where the piezoelectric coefficient d_{33} as a function of the voltage was taken from the manufacturer website (http://www.inostek.com). Our current version of the device was not optimized for high speed operation (e.g., we used very large electrodes, practically increasing the capacitance of the device). Yet, we verified the real time operation of the device by applying a square wave electrical signal at 1 kHz. The optical response followed the electrical signal, with rise time of about 100 μs, limited by the rise time of our detector. We believe that further optimization of the device can lead to operation rates in the MHz regime and even further towards the GHz. For example, the generation of GHz sound waves in PZT was previously demonstrated.[12]

Figure 4 presents the transmission spectrum of the microring under an applied voltage of 4 V not only in the forward direction, i.e., when the DC voltage was increased but also in the backward direction, i.e., when the DC voltage was decreased. One can observe a difference in the obtained wavelength shift. This indicates that the response to the applied voltage depends on its previous state. Using the relation $\Delta\lambda/\lambda_0 = \Delta n_{eff}/n_{eff}$, the performances of the presented bistable phase shifter can be evaluated. Figure 5 presents the refractive index change as a function of the applied voltage, when it is increased and decreased. The value of n_{eff} which is needed in order to perform the translation from wavelength shift into change in refractive index was taken from the electromagnetic simulation. A hysteresis behavior can be clearly observed. This nonlinear response to the applied voltage is due to the piezoelectric properties of the piezoelectric material. The nonlinear strain behavior induced by the PZT is observed in refractive index change of the optical mode because of the photoelastic effect which is assumed to be linear, under application of weak strain magnitude. Nonlinearities in the silicon waveguide are neglected because of the

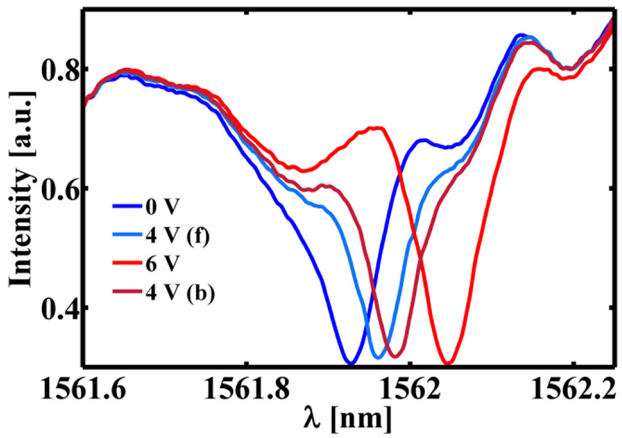

FIG. 4. Transmission spectra of the microring resonator under different voltages. The spectrum at 4 V is presented in forward direction (f) and in the backward direction (b).

relatively low optical power used in the experiment. The optical power inside the microring resonator was estimated to be about 130 μW, which is significantly smaller than the optical power reported in other works demonstrating bistability in silicon microring resonators.[11,15]

Since the nonlinear response of the presented phase-shifter has its origin in the piezoelectric properties of the PZT, bistable operation can be achieved regardless of optical input power, as long as the optical power level is below the nonlinear regime of the silicon itself. Moreover, there is no need to change the level of the input optical power in order to switch between different states. This offers a clear advantage for the application of optical memory, where the level of optical power may fluctuate. Generally speaking, when considering optical memory, one is typically considering the case of all optical memory,[10,11] i.e., optical "write" and optical "read." However, as discussed in Ref. 16, electro optic memories combining optical "write" and electrical "read" or electrical "write" and optical "read" (as in our work) exist as well. Specifically, for applications involving optical signals, the electrical "write"-optical "read" may be advantageous compared with the alternative of using an electronic memory in optical systems by electrically driving an optical source or

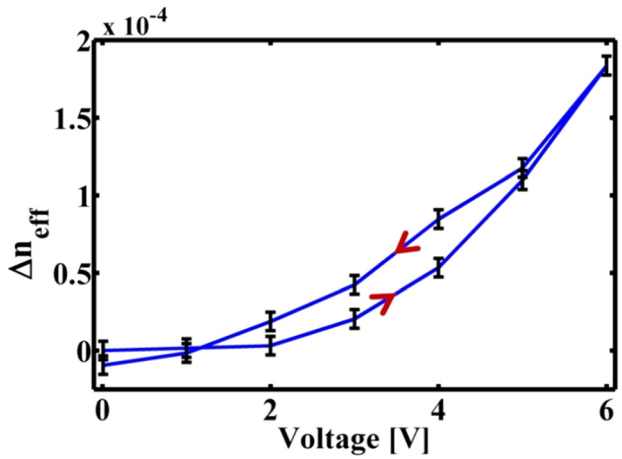

FIG. 5. Normalized shift in resonance wavelength as a function of applied voltage on the PZT.

a modulator, because it avoids the need for electro optic and opto-electronic conversions.

Here, we use the hysteresis to write a state electrically, and we read it optically by monitoring the transmission of light through the device. Depending on the history of the applied electric field, we can get either high or low transmission of light. As an example, the resonator can be connected to a DC voltage (e.g., 4 V), and the optical transmission at a specific wavelength is monitored. We write a bit of memory by applying a short voltage pulse in addition to the DC. The resulted optical transmission can be either high or low, depending on the polarity of the pulse. If the polarity is positive, the pulse voltage is added to the DC such that the total voltage goes up and falls back to 4 V. This scenario corresponds to the upper branch of the hysteresis loop. Alternatively, if the polarity is negative, the total voltage is reduced and then goes up again to 4 V, corresponding to the lower branch of the hysteresis loop, resulted in different transmission compared with the first case.

In conclusion, we demonstrated a method that allows to achieve bistability in a silicon microring resonator without involving nonlinear effects based on change in the optical power. Bistable operation was achieved using the photoelastic effect in order to take advantage of the hysteresis strain behavior of the piezoelectric material. The nonlinear strain magnitude was electrically controlled by an integrated piezoelectric sol-gel PZT thin film transducer deposited on top of the device. While the nonlinear behavior of the device depends on the intrinsic properties of the piezoelectric material, its effect on the optical mode via the photoelastic effect depends on the geometry of the cladding layer. In the presented geometry, a refractive index change of about 1.8×10^{-4} was measured under an applied voltage of 6 V.

The authors acknowledge technical support from Noa Mazursky. The research was supported in parts by the Israeli Science Foundation. Ilya Goykhman and Boris Desiatov acknowledge the Eshkol fellowship from the Israeli Ministry of Science and Technology. The devices were fabricated at the Center for Nanoscience and Nanotechnology, The Hebrew University of Jerusalem.

[1]D. J. Lockwood and L. Pavesi, *Silicon Photonics II* (Springer, Berlin, 2011), Chap. II.
[2]M. Huang, Int. J. Solids Struct. **40**, 1615–1632 (2003).
[3]D.-X. Xu, P. Cheben, D. Dalacu, A. Delage, S. Janz, B. Lamontagne, M. J. Picard, and W. N. Ye, Opt. Lett. **29**, 2384–2386 (2004).
[4]D.-X. Xu, S. Janz, and P. Cheben, IEEE Photon. Technol. Lett. **18**, 343–345 (2006).
[5]K. Voigt, L. Zimmermann, G. Winzer, T. Mitze, J. Bruns, K. Petermann, B. Huttl, and C. Schubert, IEEE Photon. Technol. Lett. **20**, 614–616 (2008).
[6]R. S. Jacobsen, K. N. Andersen, P. I. Borel, J. Fage-Pedersen, L. H. Frand-sen, O. Hansen, M. Kristensen, A. V. Lavrinenko, G. Moulin, H. Ou, C. Peucheret, B. Zsigri, and A. Bjarklev, Nature (London) **441**, 199 (2006).
[7]B. Chmielak, M. Waldow, C. Matheisen, C. Ripperda, J. Bolten, T. Wahlbrink, M. Nagel, F. Merget, and H. Kurz, Opt. Express **19**, 17212–17219 (2011).
[8]K. Tsia, S. Fathpour, and B. Jalali, Appl. Phys. Lett. **92**, 061109 (2008).
[9]A. C. Walker, Appl. Opt. **25**, 1578 (1986).
[10]M. Notomi, A. Shinya, S. Mitsugi, G. Kira, E. Kuramochi, and T. Tanabe, Opt. Express **13**, 2678–2687 (2005).
[11]V. R. Almeida and M. Lipson, Opt. Lett. **29**, 2387–2389 (2004).
[12]N. Izyumskaya, Y. I. Alivov, S. J. Cho, H. Morkoc, H. Lee, and Y. S. Kang, Crit. Rev. Solid State Mater. Sci. **32**, 111–202 (2007).
[13]K. Iniewski, *Integrated Microsystems: Materials, MEMs, Photonics, Bio Interfaces* (CRC, Vancouver, 2011), Chap. XXXII.
[14]E. D. Palik, *The Handbook of Optical Constants of Solids III* (Academic, San Diego, 1998), p. 314.
[15]P. Sun and R. M. Reano, Opt. Lett. **35**, 1124–1126 (2010).
[16]H. Coy, R. Cabrera, N. Sepúlveda, and F. E. Fernández, J. Appl. Phys. **108**, 113115 (2010).